Available online at www.sciencedirect.com
ScienceDirect
International Journal of Thermal Sciences 47 (2008) 1012–1019
International Journal of Thermal Sciences
www.elsevier.com/locate/ijts

# Optimum wall conductance ratio in magnetoconvective flow in a long vertical rectangular duct

Guillermo Ibáñez [a], Sergio Cuevas [b,*]

[a] *Universidad Politécnica de Chiapas, Tuxtla Gutiérrez, Chiapas 29010, Mexico*
[b] *Centro de Investigación en Energía, Universidad Nacional Autónoma de México, A.P. 34, Temixco, Mor. 62580, Mexico*

Received 13 April 2007; received in revised form 4 September 2007; accepted 13 September 2007
Available online 25 October 2007

**Abstract**

The entropy generation minimization method is applied to the optimization of a buoyancy-driven laminar magnetohydrodynamic flow in a long vertical rectangular duct with thin conducting or insulating walls. The flow takes place under a strong uniform magnetic field applied transversally to one pair of walls and is driven by a known constant temperature gradient aligned with the field. Numerical solutions for the velocity and electric current density in both fluid and walls are calculated using a spectral collocation method. It is shown that an optimum value of the wall conductance ratio (i.e. the ratio of the electrical conductance of the wall to that of the fluid) that minimizes the global entropy generation rate can be found. The analysis of the irreversibilities caused by heat conduction, viscosity and Joule dissipation allows to explain the existence of the optimum value.


*Keywords:* Optimization; Entropy generation; Magnetohydrodynamic flows; Free convection

## 1. Introduction

Magnetohydrodynamic (MHD) free convection flows are of considerable interest due to their frequent occurrence in applications such as crystal growth, metal casting and, in particular, liquid–metal cooled blankets for fusion reactors. In fact, the analysis of buoyancy-driven MHD flows in long vertical ducts is relevant for the separately cooled liquid–metal breeder concepts [1,2]. Unlike self-cooled blankets where buoyant effects are negligible in comparison with the forced flow driven by a high-pressure head, in the separately cooled liquid–metal breeder concepts the liquid metal is used mainly as a breeding material and the flow induced by non-uniform thermal conditions may be dominant in comparison with the forced flow. Bühler [1] performed an extensive analysis of buoyancy-driven laminar MHD flows in long vertical ducts with rectangular cross section, considering duct walls of arbitrary conductivity. Using asymptotic analysis, he derived solutions for general temperature distributions assuming that a strong uniform magnetic field is aligned with one pair of walls. Typical flow subregions, namely, the inviscid core, and Hartmann and side layers, were identified. Among other interesting results, he found high-velocity jets along perfectly conducting sidewalls. Tagawa et al. [2] have also considered the buoyant MHD flow in a long vertical enclosure of square cross section assuming that the duct is electrically insulated. For the fully developed case, they found an exact analytical solution in the central region assuming that the temperature distribution is only determined by heat conduction. Through an analytical modelling of the Hartmann layers they were able to establish boundary conditions for both the core and the side layer flows. In a second paper [3], the same authors analyzed the problem both experimentally and numerically considering the finite size of the vertical enclosures in order to determine the inertial effects on the flow. The magnetoconvective flow problem in a long vertical duct of square cross-section and arbitrary conductivity has also been numerically investigated by Di Piazza and Bühler with a finite volume method [4].

In the present contribution, the buoyancy-driven MHD flow in a long vertical rectangular duct is analyzed from an opti-

* Corresponding author. Tel.: +52 (55) 56 22 9713; fax: +52 (777) 325 00 18.
*E-mail address:* scg@cie.unam.mx (S. Cuevas).

1290-0729/$ – see front matter 
doi:10.1016/j.ijthermalsci.2007.09.003

**Nomenclature**

| | |
|---|---|
| $a$ | aspect ratio of the duct |
| $\mathbf{B}(B_o)$ | magnetic induction (module)..... tesla |
| $c$ | wall conductance ratio, $\sigma_w t_w/\sigma L$ |
| $C$ | specific heat..... $\mathrm{J\,kg^{-1}\,K^{-1}}$ |
| $Ec$ | Eckert number, $U_0^2/\Delta T C$ |
| $F$ | dimensionless potential function |
| $g$ | acceleration of gravity ..... $\mathrm{m\,s^{-2}}$ |
| $Gr$ | Grashof number, $\beta g \Delta T L^3/\nu^2$ |
| $h$ | dimensionless electric current stream function |
| $\mathbf{j}$ | dimensionless electric current density vector, $\sigma U_0 B_0$ |
| $j_y$ | dimensionless electric current density in the $\hat{y}$-direction, $\sigma U_0 B_0$ |
| $j_z$ | dimensionless electric current density in the $\hat{z}$-direction, $\sigma U_0 B_0$ |
| $k$ | fluid thermal conductivity..... $\mathrm{W\,m^{-1}\,K^{-1}}$ |
| $L$ | characteristic length, distance between Hartmann walls..... m |
| $M$ | Hartmann number, $B_0 L\sqrt{\sigma/\rho\nu}$ |
| $p$ | dimensionless pressure, $\sigma U_0 B_0^2 L$ |
| $Pe$ | Péclet number, $\rho C U_0 L/k$ |
| $Pr$ | Prandtl number, $\rho C \nu/k$ |
| $Q$ | dimensionless volumetric heat source, $k\Delta T/L^2$ |
| $Rm$ | magnetic Reynolds number, $\mu\sigma U_0 L$ |
| $\dot{S}$ | dimensionless local entropy generation rate per unit length, $k/L^2$ |
| $\langle\dot{S}\rangle$ | dimensionless global entropy generation rate per unit length |
| $T$ | dimensionless fluid temperature, $\Delta T$ |
| $T_d$ | dimensional fluid temperature ..... K |
| $T_0$ | reference temperature..... K |
| $t_w$ | wall thickness ..... m |
| $\mathbf{u}$ | dimensionless fluid velocity vector, $U_0$ |
| $u$ | dimensionless axial fluid velocity, $U_0$ |
| $U_o$ | characteristic velocity of the fluid, $\rho\beta g\Delta T/\sigma B_0^2$..... $\mathrm{m\,s^{-1}}$ |
| $x$ | dimensionless axial coordinate in the direction of acceleration of gravity, $L$ |
| $y$ | dimensionless transversal coordinate in the direction of the magnetic field, $L$ |
| $\hat{\mathbf{y}}$ | unit vector in the $y$-direction |
| $z$ | dimensionless transversal coordinate, $L$ |

*Greek symbols*

| | |
|---|---|
| $\beta$ | thermal expansion coefficient ..... $\mathrm{K^{-1}}$ |
| $\Delta T$ | characteristic temperature difference ..... K |
| $\phi$ | dimensionless electric potential, $U_0 B_0 L$ |
| $\mu$ | magnetic permeability of the fluid.. $\mathrm{m\,kg\,s^{-2}\,A^{-2}}$ |
| $\nu$ | kinematic viscosity of the fluid..... $\mathrm{m^2\,s^{-1}}$ |
| $\sigma$ | electrical conductivity of the fluid..... $\mathrm{mho\,m^{-1}}$ |

*Subscripts*

| | |
|---|---|
| $w$ | wall |
| opt | optimum |

mization point of view. The optimization criterium is the minimization of the entropy generation rate. In the context of the classical thermodynamics of irreversible processes [5] stationary non-equilibrium states are characterized by a minimum of the entropy production, compatible with the external constraints imposed on the system, provided that phenomenological coefficients are assumed constant. For the optimization and modelling of engineering devices, Bejan [6,7] has proposed the Entropy Production Minimization method in which the main idea is to carry out the optimization process with the physical constraints imposed by the irreversibilities produced by the operating device. This ensures that the intrinsic irreversibilities associated with a given physical process reach a minimum consistent with the constraints demanded by the system. This optimization method has been applied in a number of heat transfer and fluid flow problems [7–9] as well as in flows of electrically conducting fluids under magnetic fields [10–13]. In particular, Mahmud et al. [12] addressed the analysis of the entropy generation in a mixed convection channel flow under a transverse magnetic field as well as in an MHD free convection flow in a porous square cavity [13].

In this paper, the entropy generation minimization method is used to determine an optimum value of the wall conductance ratio that minimizes the global entropy generation rate. This important parameter is the ratio of the electrical conductance of the wall to that of the fluid and establishes, to a great extent, the dynamic behavior of the flow. In fact, it determines, along with the Hartmann number, the amount of current that circulates in the fluid and the duct walls. We use a numerical approach to calculate the velocity and electric current density fields in a long vertical duct of rectangular cross-section subjected to a known constant temperature gradient. A very efficient spectral collocation method, previously applied to the study of pressure driven MHD flows [14,15], is used for the flow analysis in ducts with wall conductance ratios ranging from insulating to thin conducting. A composite core-side-layer solution allows an explicit resolution of the fully developed flow in the side layers even for Hartmann numbers as high as $10^4$. Although not resolved explicitly, Hartmann layers are considered as a return path for electrical currents. Once the MHD problem is solved, the local and global entropy generation rate that considers the irreversibilities caused by heat flow, fluid friction, and ohmic or Joule dissipation in both fluid and duct walls are calculated. Further, the global entropy generation rate is minimized as a function of the wall conductance ratio. The existence of the minimum value is explained by looking at the dissipative behavior of the flow.

## 2. Formulation

We consider the buoyancy-driven flow of a liquid metal in a long vertical duct of constant rectangular cross-section under the action of a strong, uniform, horizontal magnetic field. It is assumed that the duct's axis lies in the $x$-direction (the direction of the acceleration of gravity) while the magnetic field points in the $y$-direction, $\mathbf{B} = B_o\hat{\mathbf{y}}$, being parallel to two of the duct's walls. Here $B_o$ and $\hat{\mathbf{y}}$ are the strength of the field and the unit vector in the $y$-direction, respectively. We assume the existence of a constant temperature gradient between the walls transversal to the field. Therefore, a heat flux antiparallel to the horizontal magnetic field is produced. A sketch of the problem is shown in Fig. 1. The temperature difference between the walls originates a convective motion of the fluid in the vertical direction. Moreover, due to the motion of the fluid in the magnetic field, closed current loops in the $yz$-plane, normal to the axial motion, are induced. Electric currents can circulate either in the fluid or in the fluid and walls, according to the relative electrical conductivity of the fluid and walls. We assume the magnetic Reynolds number, $Rm = \mu\sigma U_o L$, to be much less than unity so that the magnetic field induced by electric currents is neglected. Here $\mu$ and $\sigma$ are the magnetic permeability and electrical conductivity of the fluid, respectively, while $U_o$ and $L$ are the characteristic velocity and length of the flow, respectively. In this problem, $L$ is taken as half the distance between the walls of the duct parallel to the magnetic field.

Under very strong magnetic fields, the flow region splits into a core surrounded by thin viscous boundary layers. The layers formed near the walls perpendicular to the externally applied magnetic field are called the Hartmann layers, while those near the walls parallel to the magnetic field are called the side layers. The present analysis is based on the thin conducting wall approximation, expressed by the condition $M^{-1} \ll c \ll 1$ [14]. Here, $c = \sigma_w t_w/\sigma L$ is the wall conductance ratio which expresses the ratio of the electrical conductance of the wall to that of the fluid while $M = B_o L\sqrt{\sigma/\rho\nu}$ is the Hartmann number which estimates the magnetic forces compared with viscous forces; $\sigma_w$ and $t_w$ are the electrical conductivity and thickness of the wall, respectively, while $\rho$ and $\nu$ are the mass density and kinematic viscosity of the fluid, respectively. In this work, the conductivities of all walls are assumed to be the same but different wall conductivities may also be considered.

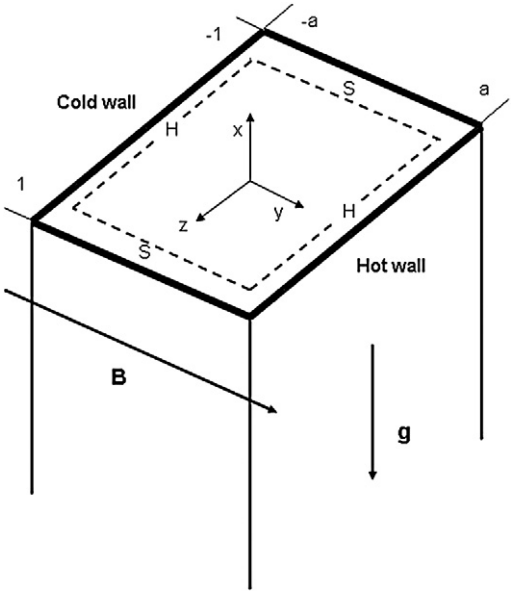


Fig. 1. Sketch of the vertical duct with a uniform magnetic field antiparallel to the heat flux ($T = y$). Dotted lines illustrate Hartmann ($H$) and side ($S$) layers.

The dimensionless system of equations governing the stationary buoyant magnetohydrodynamic flow of a liquid metal immersed in a magnetic field is expressed as [1]

$$\nabla \cdot \mathbf{u} = 0 \tag{1}$$

$$\frac{Gr}{M^4}(\mathbf{u}\cdot\nabla)\mathbf{u} = -\nabla p + \frac{1}{M^2}\nabla^2\mathbf{u} + \mathbf{j}\times\hat{\mathbf{y}} + T\hat{\mathbf{x}} \tag{2}$$

$$Pe(\mathbf{u}\cdot\nabla)T = \nabla^2 T + Q \tag{3}$$

$$\mathbf{j} = -\nabla\phi + \mathbf{u}\times\hat{\mathbf{y}} \tag{4}$$

$$\nabla\cdot\mathbf{j} = 0 \tag{5}$$

where the velocity $\mathbf{u}$, the pressure $p$, the electric current density $\mathbf{j}$, the electric potential $\phi$ and the volumetric heat source $Q$, are normalized by $U_0 = \rho\beta g\Delta T/\sigma B_0^2$, $\sigma U_0 B_0^2 L$, $\sigma U_0 B_0$, $U_0 B_0 L$ and $k\Delta T/L^2$, respectively. Here $T$ stands for the difference between the dimensional local temperature $T_d$ and a reference temperature $T_0$, normalized by a characteristic temperature difference $\Delta T$. In addition, $g$, $k$ and $\beta$ are, respectively, the magnitude of the gravitational acceleration, the thermal conductivity and the thermal expansion coefficient according to the Boussinesq approximation. The applied magnetic field is normalized by $B_0$ while all length dimensions are normalized by $L$. The conservation of mass is expressed through Eq. (1). In turn, the balances of momentum and energy are given by Eqs. (2) and (3), respectively. In addition, Ohm's law is given by Eq. (4) while electric charge conservation is expressed through Eq. (5). For the solution of the previous system of equations we follow the approach presented in [14] for pressure driven MHD flows.

## 3. Temperature, velocity and electrical current density fields

As stated by Bühler [1], in general when working fluids with very high thermal conductivity such as liquid metals and semiconductors are considered, the convective heat flux can be neglected if $Pe \ll 1$. Under these conditions, the temperature field becomes independent of the flow and can be determined by solving $\nabla^2 T = -Q$ with suitable boundary conditions. Since we assume that the duct is long enough so that the flow is unidirectional, thermally fully developed conditions hold and the conductive solution is also valid. Here we consider that the volumetric heat flux is zero and that a constant heat flux crosses the duct between the Hartmann walls at $y = -a$ (cold wall) and $y = a$ (hot wall), where $a$ is the duct's aspect ratio, so that the temperature field can be expressed as $T = y$ [1]. Therefore, the heat flux is antiparallel to the applied magnetic field $\mathbf{B}$. In turn, the side walls at $z = -1$ and $z = 1$ are assumed to be adiabatic. We also assume that there is no externally applied pressure gradient so that the flow is driven by pure buoy-

ancy. In general, for large Hartmann number flows such that $Gr/M^4 \ll 1$, inertia effects can be neglected in the momentum balance equation (2). In the present case, as stated above, we assume that the duct is long enough and fully developed flow conditions are also established. Hence, all functions are independent of the $x$-coordinate, in particular, $\partial p/\partial x = 0$. Therefore, the problem becomes two-dimensional with $\mathbf{u} = [u(y,z), 0, 0]$ and $\phi = \phi(y,z)$. Under these conditions, the simplified governing equations are:

$$0 = \frac{1}{M^2}\left(\frac{\partial^2 u}{\partial y^2} + \frac{\partial^2 u}{\partial z^2}\right) + \frac{\partial \phi}{\partial z} - u + T \tag{6}$$

$$j_y = -\frac{\partial \phi}{\partial y}, \qquad j_z = -\frac{\partial \phi}{\partial z} + u \tag{7}$$

$$\frac{\partial j_y}{\partial y} + \frac{\partial j_z}{\partial z} = 0 \tag{8}$$

where Eq. (6) establishes the balance among viscous, magnetic and buoyant forces. At the walls, we have to satisfy Ohm's law and current conservation

$$j_{yw} = -\left(\frac{\sigma_w}{\sigma}\right)\frac{\partial \phi_w}{\partial y}, \qquad j_{zw} = -\left(\frac{\sigma_w}{\sigma}\right)\frac{\partial \phi_w}{\partial z} \tag{9}$$

$$\frac{\partial j_{yw}}{\partial y} + \frac{\partial j_{zw}}{\partial z} = 0 \tag{10}$$

where the subindex $w$ denotes a property or variable of the wall.

Eqs. (8) and (10) allow the elimination of the electric current density by introducing the electric current stream functions $h$ and $h_w$ for the fluid and wall, respectively, defined as

$$j_y = -\frac{\partial h}{\partial z}, \qquad j_z = \frac{\partial h}{\partial y} \tag{11}$$

$$j_{yw} = -\frac{\partial h_w}{\partial z}, \qquad j_{zw} = \frac{\partial h_w}{\partial y} \tag{12}$$

In terms of $h$ and $h_w$, Ohm's law in the fluid and walls, Eqs. (7) and (9), respectively, can be rewritten as

$$\frac{\partial h}{\partial z} = \frac{\partial \phi}{\partial y}, \qquad \frac{\partial h}{\partial y} + \frac{\partial \phi}{\partial z} = u \tag{13}$$

$$\frac{\partial h_w}{\partial z} = \left(\frac{\sigma_w}{\sigma}\right)\frac{\partial \phi_w}{\partial y}, \qquad \frac{\partial h_w}{\partial y} + \left(\frac{\sigma_w}{\sigma}\right)\frac{\partial \phi_w}{\partial z} = 0 \tag{14}$$

Since $\partial\phi/\partial y = \partial h/\partial z$, a suitable potential function $F(y,z)$ can be introduced for $h$ and $\phi$, defined in the following way

$$h = \frac{\partial F}{\partial y}, \quad \phi = \frac{\partial F}{\partial z} \tag{15}$$

and, similarly, for the wall we have

$$h_w = \frac{\partial F_w}{\partial y}, \qquad \phi_w = \frac{\partial F_w}{\partial z} \tag{16}$$

Using (11) and (15), Eq. (6) becomes

$$0 = \frac{1}{M^2}\left(\frac{\partial^2 u}{\partial y^2} + \frac{\partial^2 u}{\partial z^2}\right) - \frac{\partial^2 F}{\partial y^2} + T \tag{17}$$

Further, note that from Eqs. (13) and (15), we have

$$u = \frac{\partial^2 F}{\partial y^2} + \frac{\partial^2 F}{\partial z^2} \tag{18}$$

so that Eq. (17) can be fully expressed in terms of $F$ and $T$. In turn, Ohm's law and current conservation at the wall can be expressed in terms of $F_w$. Eq. (17) can be solved provided that $T$ is known and suitable boundary conditions are given. As we previously mentioned, we consider a constant heat flux aligned with the applied magnetic field $\mathbf{B}$ so that the temperature field is expressed as $T = y$. For the given temperature field, the velocity distribution is an odd function of $y$ and an even function of $z$. Due to the symmetry conditions, we need to consider only one quarter of the duct's cross-section. The formulation of the boundary conditions for the present problem is the same as in [14], therefore, details will be avoided here. The idea is to decouple the electric current density and electric potential function of the fluid, walls and surrounding medium, using the thin wall approximation. That is, the walls are assumed to be thin, $t_w \ll L$, and the surrounding medium is assumed to be an electrical insulator. With these assumptions a boundary condition for the fluid variables at the inside surface of each wall can be derived, and the whole problem can be formulated in terms of the potential function $F$. In particular, it can be shown that continuity conditions at the fluid-wall interface, lead to the relation [14]

$$F_w = F(y,1) = -c\frac{\partial F}{\partial z}(y,1) \tag{19}$$

so that once $F$ is determined electric currents in the walls can be calculated using Eqs. (12), (16), and (19).

The duct flow is resolved using a composite core-side-layer solution in which the core and side layer are treated as a single solution which occupies the region $0 \leqslant y \leqslant a$, $0 \leqslant z \leqslant 1$ [14]. Since $M$ is assumed to be sufficiently large, the Hartmann layers and corner regions are ignored in the sense that they are not resolved numerically and the non-slip condition at the Hartmann walls is not satisfied. Nevertheless, Hartmann layers are considered as a return path for electric currents. This means that the amount of current that flows through these layers and, consequently, its contribution to the entropy generation rate, are properly calculated within the limits of the approximation. This approach presents the advantage that, while considering the main dynamic and dissipative effects of the Hartmann layers, the extremely expensive numerical resolution of these layers is avoided. In fact, velocity is properly calculated everywhere except within a distance $O(M^{-1})$ of the Hartmann walls. On the other hand, the side layers, where strong jets are formed, are fully resolved. Within the former approximations, the equation that satisfies the potential $F$ in the region $0 \leqslant y \leqslant a$ and $0 \leqslant z \leqslant 1$, is

$$\frac{\partial^2 F}{\partial y^2} - \frac{1}{M^2}\left(\frac{\partial^4 F}{\partial y^4} + 2\frac{\partial^4 F}{\partial y^2 \partial z^2} + \frac{\partial^4 F}{\partial z^4}\right) = y \tag{20}$$

and the boundary conditions are [14]

$$\frac{\partial^3 F}{\partial y \partial z^2} = 0, \quad \frac{\partial F}{\partial y} = 0 \quad \text{at } y = 0 \tag{21}$$

$$\frac{\partial^3 F}{\partial z^3} = 0, \quad \frac{\partial F}{\partial z} = 0 \quad \text{at } z = 0 \tag{22}$$

$$\frac{\partial F}{\partial y} - \left(c + M^{-1}\right)\frac{\partial^2 F}{\partial z^2} = M^{-1}\frac{\partial^2 F}{\partial y^2} \quad \text{at } y = a \tag{23}$$

$$\frac{\partial^2 F}{\partial y^2} + \frac{\partial^2 F}{\partial z^2} = 0, \quad F + c\frac{\partial F}{\partial z} = 0 \quad \text{at } z = 1 \tag{24}$$

In addition, the volume flux conservation condition has to be satisfied. The system of Eqs. (20)–(24) is solved numerically with a spectral collocation method [14,16], expressing the unknown function $F$ as a finite series in terms of Chebyshev polynomials, namely,

$$F(y,z) = \sum_{l=0}^{NY}\sum_{n=0}^{NZ} A_{ln} T_{2l}(y/a) T_{2n}(z)$$

where $A_{nl}$ are coefficients to be determined and $T_{2l}(y/a)$ and $T_{2n}(z)$ are odd and even Chebyshev polynomials of order $2l$ and $2n$, respectively. $NY$ and $NZ$ are the truncation limits in the Chebyshev series in $y$ and $z$, respectively. In order to reduce the system of partial differential equations to a system of simultaneous linear algebraic equations for the coefficients $A_{ln}$, Gauss–Lobatto collocation points are used [16]:

$$y_i = a\cos\left(\frac{i\pi}{2NY}\right), \quad \text{for } i = 0 \text{ to } NY$$

$$z_k = \cos\left[\frac{k\pi}{2(NZ-1)}\right], \quad \text{for } k = 0 \text{ to } (NZ-1)$$

These points yield a good numerical resolution for the boundary layers by concentrating points near the walls. The system of simultaneous algebraic equations for the coefficients $A_{ln}$ of the series is solved with the Gauss–Jordan elimination method. Numerical results for pressure-driven MHD flows obtained with this solution procedure [14] show a reasonable agreement with experimental results [17].

For the case of buoyant MHD flows, results have been verified by comparison with flow patterns obtained by Bühler [1] under different thermal conditions, where the governing equations were solved using asymptotic expansions and finite differences. Fig. 2 shows the velocity distribution for the buoyant flow in a square duct ($a = 1$) for $c = 0.05$ and $M = 1000$. The velocity displays the typical characteristics of this kind of convective MHD flows [1]. It is observed that strong jets appear in the viscous side layers while inviscid layers are also formed in the core. Since hot and cold walls are located at $y = 1$ and $y = -1$, respectively, the jet velocity in the side layers is positive for $y > 0$, while it is negative for $y < 0$. For small values of the wall conductance ratio all flow is carried by the viscous and inviscid layers and the rest of the core remains almost stagnant [1].

## 4. Entropy generation rate

Let us now calculate the entropy generation rate for the magnetoconvective flow. When irreversibilities caused by heat transfer, fluid friction and electric conduction are considered [5], the local entropy generation rate per unit length, $\dot{S}$, can be expressed in dimensionless form as

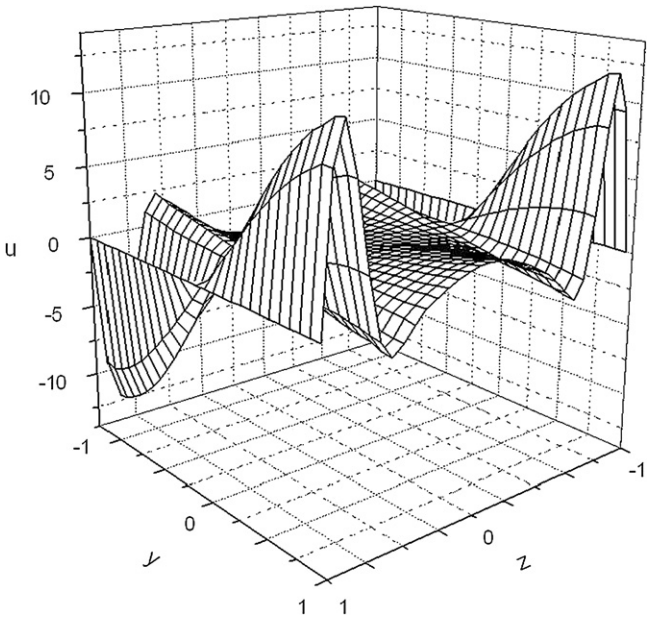


Fig. 2. Axial velocity as a function of coordinates $y$ and $z$ for the buoyant MHD flow in a vertical square duct. $M = 1000$, $c = 0.05$.

$$\dot{S} = \frac{1}{(T+\widehat{T}_o)^2}\left(\frac{\partial T}{\partial y}\right)^2 + PrEc\left\{\frac{1}{T+\widehat{T}_o}\left[\left(\frac{\partial u}{\partial y}\right)^2 + \left(\frac{\partial u}{\partial z}\right)^2\right] + \frac{M^2}{T+\widehat{T}_o}\left(j_y^2 + j_z^2\right) + \frac{M^2}{\widehat{T}_o}\frac{t_w/L}{c}\left(j_{wy}^2 + j_{wz}^2\right)\right\} \tag{25}$$

where $\dot{S}$ is normalized by $k/L^2$. Here, $Pr = \rho C\nu/k$ and $Ec = U_o^2/\Delta TC$ are the Prandtl and Eckert numbers, respectively, and $\widehat{T}_o = T_o/\Delta T$ is the dimensionless reference temperature. Note that the last two terms of Eq. (25) correspond to the ohmic dissipation due to electric conduction in the fluid and walls, respectively. From Eqs. (12), (16), and (19) it is found that electric currents in the walls are given by

$$j_{wy} = c\partial^3 F/\partial y\partial z^2(y,1)$$
$$j_{wz} = -c\partial^3 F/\partial y^2\partial z(y,1) \tag{26}$$

so that ohmic dissipation in the walls is zero for an insulating wall duct ($c = 0$). In addition to the wall conductance ratio, dissipation in the walls is also governed by the ratio $t_w/L$ which is assumed to be much less than unity. For numerical calculations the value $t_w/L = 0.01$ was used.

Since the temperature field is known and the velocity and electric current density components are calculated numerically, Eq. (25) can be evaluated at every point of the flow domain. In fact, once the potential $F$ is determined, the velocity is evaluated using Eq. (18) while current density components in both fluid and walls are calculated, respectively, from Eqs. (11) and (15), and Eqs. (26). In Figs. 3(a) and 3(b), the local entropy generation rate (25) for $c = 0$ and $c = 0.04$, respectively, is shown in one quarter of the duct ($0 \leqslant y \leqslant 1$, $0 \leqslant z \leqslant 1$) as a function of coordinates $y$ and $z$. Both figures correspond to $M = 1000$, $\widehat{T}_o = 300$ and the product $Pr \times Ec = 10^{-6}$. This value is obtained using the physical properties of liquid mercury at 27 °C which was chosen because its common use in laboratory experiments. In fact, it was found that the qualitative behavior of

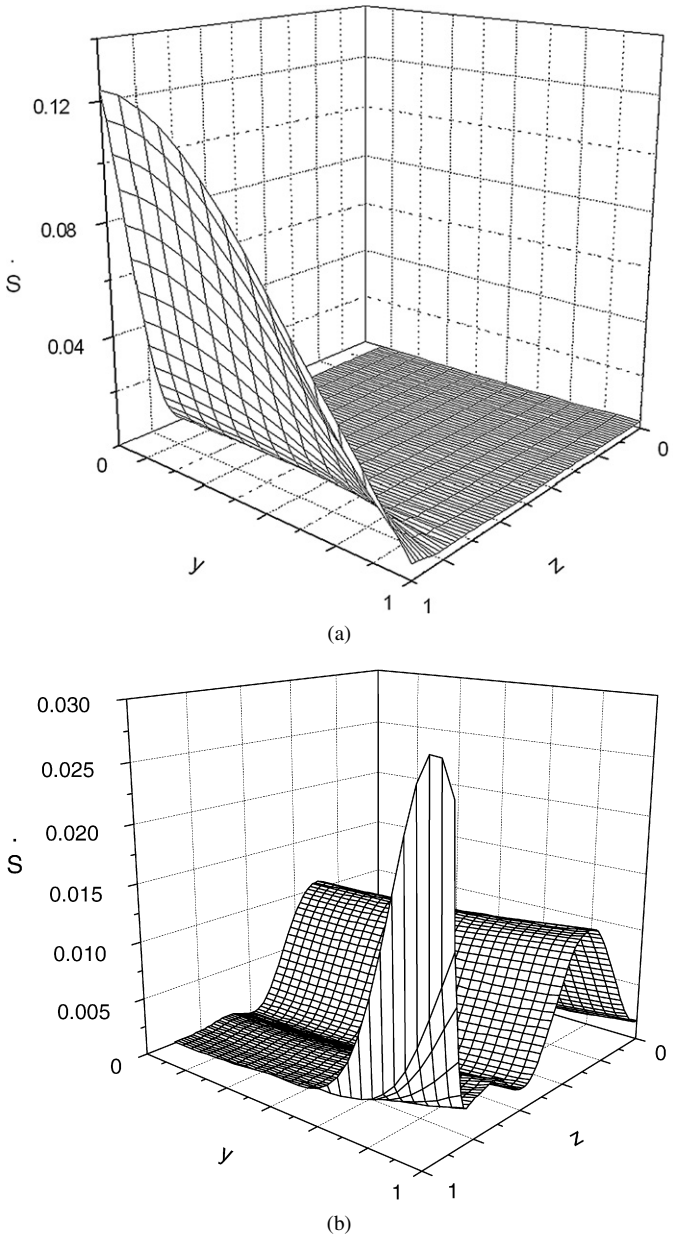


Fig. 3. (a) Local entropy generation rate, $\dot{S}$, as a function of coordinates $y$ and $z$ in the buoyant MHD flow in a vertical square duct with insulating walls. $M = 1000$, $c = 0$, $Pr \times Ec = 10^{-6}$, $\widehat{T}_o = 300$. (b) Local entropy generation rate, $\dot{S}$, as a function of coordinates $y$ and $z$ in the buoyant MHD flow in a vertical square duct with thin conducting walls. $M = 1000$, $c = 0.04$, $t_w/L = 0.01$, $Pr \times Ec = 10^{-6}$, $\widehat{T}_o = 300$.

the entropy generation rate is not very sensitive to parameters $\widehat{T}_o$ and $Pr \times Ec$. For all calculations, we considered a duct of square cross-section ($a = 1$). The analysis of the local entropy generation rate allows to determine the dissipative behavior of the system. For instance, Fig. 3(a) shows that for an insulating wall duct ($c = 0$) dissipation is concentrated in the side layers, that is, $\dot{S}$ takes high values in this region compared with the core flow where it is close to zero. On the other hand, for a thin conducting wall ($c = 0.04$), Fig. 3(b) shows that dissipation is strongly concentrated in the core flow although a noticeable increase is observed near the corner of the duct. Here, due to

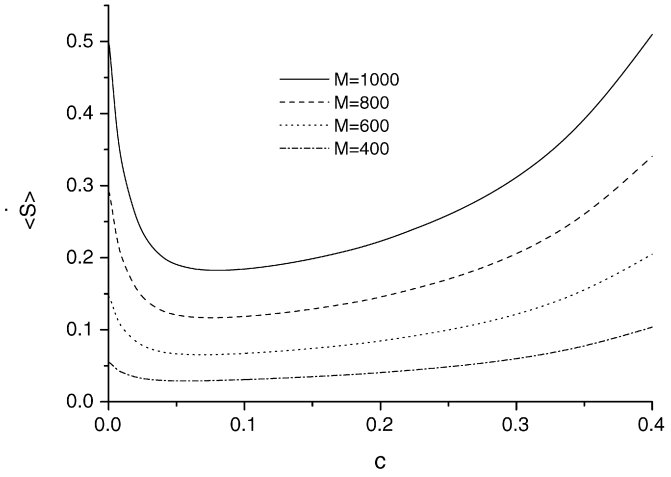


Fig. 4. Global entropy generation rate, $\langle \dot{S} \rangle$, as a function of wall conductance ratio, $c$, for different values of the Hartmann number, $M$, in the buoyant MHD flow in a vertical square duct. $t_w/L = 0.01$, $Pr \times Ec = 10^{-6}$, $\widehat{T}_o = 300$.

the high velocity jet, velocity gradients are enlarged and consequently viscous dissipation increases. Notice, however, that the highest value of the local entropy generation rate for the case $c = 0.04$ is about 20% of the highest value of $\dot{S}$ for the case $c = 0$. Therefore, dissipation is more intense in insulating than in thin conducting wall ducts.

In order to get an explicit expression of the global entropy generation rate per unit length, $\langle \dot{S} \rangle$, Eq. (25) has to be integrated in the cross-section of the duct. Once the integration is carried out, the dependence on the $y$ and $z$ coordinates disappears and $\langle \dot{S} \rangle$ becomes only a function of the relevant parameters governing the behavior of the flow, namely, $M$, $c$, $Pr$, $Ec$ and $\widehat{T}_o$. In Fig. 4, the global entropy generation rate, $\langle \dot{S} \rangle$, is presented as a function of $c$ for different $M$ values. The parameters $\widehat{T}_o$ and $Pr \times Ec$ are the same as in Figs. 3(a) and 3(b). It is observed that, for a fixed $M$, $\langle \dot{S} \rangle$ presents a minimum for a given value of $c$. The value of the minimum is higher the higher the Hartmann number. This is explained by an increase of Joule dissipation as the Hartmann number grows. The minimum expresses the fact that, for a given $M$, there is an optimum value of the wall conductance ratio that minimizes the irreversibilities associated to this MHD flow, provided the other parameters remain fixed. An explanation of the existence of this minimum can be given by looking at the dissipative behavior of the system. As it will be shown below, the behavior of the total global entropy generation rate is mainly determined by irreversibilities associated to ohmic dissipation.

Note first that the strong MHD effects that arise in high Hartmann number flows enhance the dissipation. On the one hand, as $M$ increases the velocity is reduced in the core and grows in the side-wall layer where a peak velocity appears; therefore, irreversibilities associated to viscous dissipation increase due to the steep velocity gradients (see Fig. 2). On the other hand, the electric current, which is a source of ohmic or Joule dissipation, in the liquid and walls, also increases with $M$. This means that the entropy generation rate always increases with $M$ when a constant temperature gradient aligned to **B** is imposed on the fluid. In fact, for high Hartmann numbers flows in ducts with

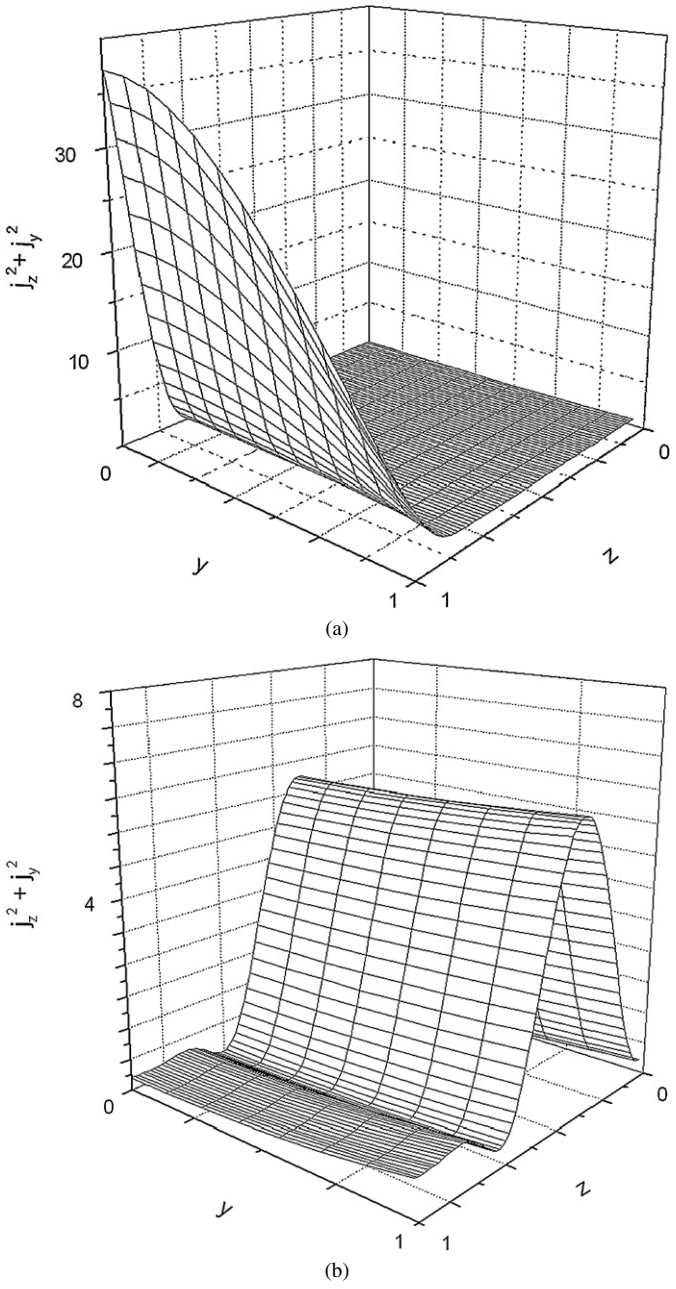


Fig. 5. (a) Ohmic dissipation ($j_y^2 + j_z^2$) as a function of coordinates $y$ and $z$ in the buoyant MHD flow in a vertical square duct with insulating walls. $c = 0$, $M = 1000$. (b) Ohmic dissipation ($j_y^2 + j_z^2$) as a function of coordinates $y$ and $z$ in the buoyant MHD flow in a vertical square duct with thin conducting walls. $M = 1000$, $c = 0.04$, $t_w/L = 0.01$.

either insulating or thin conducting walls, the contribution associated to ohmic dissipation in the total entropy generation rate dominates over the other two contributions, namely, heat conduction and fluid friction. This can be understood by looking at Figs. 5(a) and 5(b) where the ohmic dissipation in the fluid, namely the sum of the squares of $j_y$ and $j_z$, as a function of $y$ and $z$ is shown in one quarter of the duct for $c = 0$ and $c = 0.04$, respectively. In the insulating wall case (Fig. 5(a)) all the current circulates within the fluid so that current exiting the core penetrates the side layer before closing through the Hartmann layer. Hence, in this case ohmic dissipation is very strong in the side layer, as can be observed in Fig. 5(a). For conducting walls ($c \neq 0$) a fraction of the current is carried out by the walls so that the current in the boundary layers is lower compared with the insulating wall case. Also, when $c$ increases, the electric wall resistance decreases and the current in the fluid core increases. Therefore, ohmic dissipation is concentrated in the core flow, as is shown in Fig. 5(b). The qualitative correspondence of Figs. 3(a)–(b) and Figs. 5(a)–(b) shows the strong influence of ohmic dissipation in the dissipative behavior of the flow. The existence of the minimum value of $\langle \dot{S} \rangle$ can be explained as follows. For $c = 0$, the entropy generation is governed by the ohmic dissipation created by electric currents circulating in the boundary layer and reaches high values (see Fig. 3(a)). As $c$ grows, the dissipation associated to electric conduction in the boundary layers near the channel walls decreases since dissipation is enhanced in the fluid core and, consequently, $\langle \dot{S} \rangle$ decreases. However, for larger values of $c$, the enhancement of ohmic dissipation in the fluid core becomes dominant and $\langle \dot{S} \rangle$ increases.

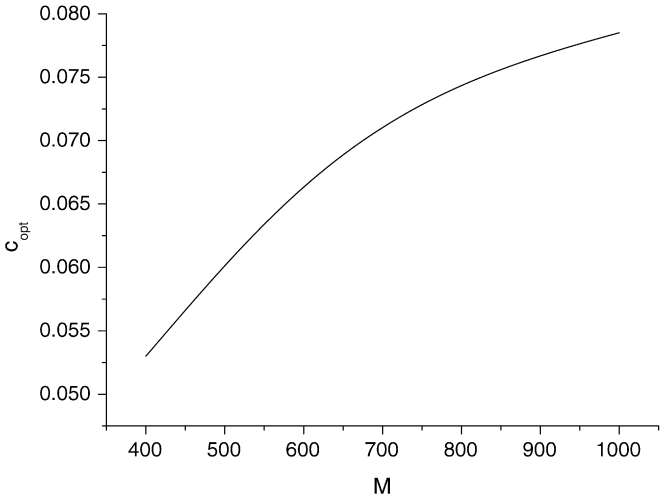


Fig. 6. Optimum wall conductance ratio, $c_{\text{opt}}$, as a function of the Hartmann number, $M$. $Pr \times Ec = 10^{-6}$, $\widehat{T}_o = 300$.

Fig. 6 shows the optimum wall conductance ratio, $c_{\text{opt}}$, as a function of $M$ for the same conditions as in previous figures. It is observed that the higher the Hartmann number, the higher $c_{\text{opt}}$. Note, however, that the optimum wall conductance ratio that minimizes $\langle \dot{S} \rangle$, seems to approach a limiting value as $M$ grows.

## 5. Conclusions

In this paper, we have shown that it is possible to find an optimum value of the wall conductance ratio that minimizes the global entropy generation rate in a buoyant magnetoconvective flow in a long vertical rectangular duct. The MHD flow was solved numerically when the applied magnetic field is transversal to the duct axis and normal to a pair of walls, while there is a constant heat flux antiparallel to the applied field. For the numerical solution, we followed an approach used for pressure driven MHD flows in ducts with thin conducting or insulating walls [14]. With a core-side-layer solution valid for high

Hartmann numbers, the velocity and the electric current density fields were determined using a spectral collocation method. These fields were used to evaluate the local and global entropy generation rate that considers irreversibilities caused by heat transfer, fluid friction and electric conduction in both fluid and walls. The transition from a thin conducting to an insulating wall duct clearly reveals that the global entropy generation rate reaches a minimum for a given wall conductance ratio, the value of which increases with the Hartmann number when the other parameters remain fixed. The existence of this minimum can be explained by analyzing the detailed dissipative flow behavior as the relevant parameters are varied. It was found that the behavior of the total global entropy generation rate is mainly determined by irreversibilities associated to ohmic dissipation.

The problem dealt with in this paper shows the kind of useful information that can be obtained from the entropy generation minimization method. In fact, from an optimum wall conductance ratio, it is possible to determine the geometry and/or materials that minimize irreversibilities for given flow conditions. The methodology presented here can be applied to optimize other MHD duct flows of practical relevance.

## Acknowledgement

The authors wish to thank Prof. M. López de Haro for valuable comments on the manuscript. Support from PAPIIT-UNAM and CONACYT-FOMIX under projects IN111705 and CHIS-2006-C06-45675, respectively, is gratefully acknowledged.

## References

[1] L. Bühler, Laminar buoyant magnetohydrodynamic flow in vertical rectangular ducts, Phys. Fluids 10 (1) (1998) 223–236.

[2] T. Tagawa, G. Authié, R. Moreau, Buoyant flow in long vertical enclosures in the presence of a strong horizontal magnetic field. Part 1. Fully established flow, Europ. J. Mech. B/Fluids 21 (2002) 383–398.

[3] G. Authié, T. Tagawa, R. Moreau, Buoyant flow in long vertical enclosures in the presence of a strong horizontal magnetic field. Part 2. Finite enclosures, Europ. J. Mech. B/Fluids 22 (2003) 203–220.

[4] I. Di Piazza, L. Bühler, A general computational approach for magnetohydrodynamic MHD flows using the CFX code: Buoyant flow through a vertical square channel, Fusion Technol. 38 (2) (2000) 180–189.

[5] S.R. De Groot, P. Mazur, Non-Equilibrium Thermodynamics, Dover, New York, 1984.

[6] A. Bejan, Entropy Generation through Heat and Fluid Flow, John Wiley and Sons, New York, 1982.

[7] A. Bejan, Entropy Generation Minimization, CRC Press, Boca Raton, 1996.

[8] G. Ibáñez, S. Cuevas, M. López de Haro, Minimization of entropy generation by asymmetric convective cooling, Int. J. Heat Mass Transfer 46 (2003) 1321–1328.

[9] G. Ibáñez, S. Cuevas, M. López de Haro, Heat transfer in asymmetric convective cooling and optimized entropy generation rate, Rev. Mex. Fís. 49 (2) (2003) 338–343.

[10] G. Ibáñez, S. Cuevas, M. López de Haro, Optimization analysis of an alternate magnetohydrodynamic generator, Energy Conversion and Management 43 (2002) 1757–1771.

[11] G. Ibáñez, M. López de Haro, S. Cuevas, Thermodynamic optimization of radial MHD flow between parallel circular disks, J. Non-Equil. Thermodynamics 29 (2004) 107–122.

[12] S. Mahmud, S.H. Tasnim, M.A.H. Mamun, Thermodynamic analysis of mixed convection in a channel with transverse hydromagnetic effect, Int. J. Thermal Sci. 47 (2003) 731–740.

[13] S. Mahmud, R.A. Fraser, Magnetohydrodynamic free convection and entropy generation in a square porous cavity, Int. J. Heat Mass Transfer 47 (2004) 3245–3256.

[14] S. Cuevas, B.F. Picologlou, J.S. Walker, G. Talmage, Liquid-metal MHD flow in rectangular ducts with thin conducting or insulating walls: Laminar and turbulent solutions, Int. J. Engrg. Sci. 35 (5) (1997) 485–503.

[15] S. Cuevas, B.F. Picologlou, J.S. Walker, G. Talmage, T.Q. Hua, Heat transfer in laminar and turbulent liquid–metal MHD flows in square ducts with thin conducting or insulating walls, Int. J. Engrg. Sci. 35 (5) (1997) 505–514.

[16] C. Canuto, M.Y. Hussani, A. Quarteroni, A.T. Zang, Spectral Methods in Fluid Dynamics, Springer-Verlag, New York, 1987.

[17] U. Müler, L. Bühler, Magnetofluiddynamics in Channels and Containers, Springer-Verlag, New York, 2001.